ISSN 1392–1320 MATERIALS SCIENCE (MEDŽIAGOTYRA). Vol. 31, No. 4. 2025

Magnetic and Mechanical Properties of $FeCoNi(CuAl)_{0.2}$ High-entropy Alloy Film

Yujian LI [1, 2], Qiqi CHEN [1], Yushan LIU [1], Rui WANG [1], Dezhi ZHU [3], Shaofeng YANG [1 *]

[1] *Tianjin Key Laboratory of High Performance Precision Forming Technology and Equipment, Tianjin University of Technology and Education, Tianjin, China*
[2] *Department of Mechanical and Electrical Engineering, Quzhou College of Technology, Quzhou, China*
[3] *Guangdong Provincial Key Laboratory for Processing and Forming of Advanced Metallic Materials, South China University of Technology, Guangzhou 510640, China*

http://doi.org/10.5755/j02.ms.39875

Received 19 December 2024; accepted 12 February 2025

$FeCoNi(CuAl)_{0.2}$ high entropy alloy (HEA) thin films were produced by magnetron sputtering. Results from X-ray diffractometry analysis, scanning electron microscopy, energy dispersive spectroscopy, and atomic force microscope indicate the formation of a single face-centered cubic solid solution with a homogenous distribution of alloying elements in the film according to the designed composition after 30 min of sputtering. The vibrant sample magnetometer test illustrated soft magnetic behavior with 139.67 emu/g magnetic saturation (MS) and 7.96 Oe coercivity field (*Hc*) in a 2 T applied magnetic field with excellent hardness 136.8 GPa and Young's modulus 7.33 GPa. The formation of micro-nano columnar crystals led to a higher MS and lower *Hc*.
Keywords: high entropy alloy film, microstructure, magnetron sputtering, magnetic properties.

1. INTRODUCTION

With the rapid developments of telecommunication technology, micromagnetic devices have the tendency to high performance, integration, and miniaturization. Therefore, soft magnetic films with higher saturation magnetization, lower coercivity and resistance to stress deformation characteristics have attracted more and more attention. Consequently, there is a growing interest in soft magnetic films that exhibit high temperature stability, corrosion resistance, and high magnetic susceptibility among researchers [1 – 4]. Certain high-entropy alloys (HEAs) are known to possess notably superior soft magnetic properties due to their high saturation magnetization (Ms), high electrical resistivity and malleability, low coercivity (*Hc*) and coupled with excellent thermal stability and corrosion resistance [5, 6]. Soft magnetic FeCoNiCrAlSi high entropy alloy film film has excellent magnetic properties, its saturation magnetization reaches 9.13 × 105 A/m, coercivity is 79.6 A/m. The $AlFeNiCoxCr_{1-x}$ alloys (x from 0 to 1) exhibits the increased Ms from 18.48 emu/g to 117.8 emu/g with the Co addition, while the Cr element reduced ferromagnetic interactions between Fe, Ni, and Co.

Many studies mainly focus on FeCoNi-based alloys and investigate how metals or nonmetals such as Nb and Cr, Al and B, Al and Si, Mn and Cu affect HEA structure and affect HEA structure and Magnetic properties. There has been less paid attention to the effect of Cu and Al as a metallic element on FeCoNi-based HEA films phase formation and magnetic properties. In additon, $FeCoNi(CuAl)_x$ alloy system shows higher saturation magnetic intensity, especially $FeCoNi(CuAl)_{0.2}$ prepared by arc melting technology. The present study aims to synthesize a soft magnetic $FeCoNi(CuAl)_{0.2}$ HEA film with high hardness employing magnetron sputtering techniques and the effect of microstructure on mechanical properties and magnetic properties of HEA magnetron sputtering films was investigated. Subsequently, a comprehensive analysis of the films microstructure, phase transitions, and mechanical and soft magnetic behavior will be conducted.

2. MATERIALS AND METHODS

The $FeCoNi(CuAl)_{0.2}$ HEA sputtering targets were fabricated via mechanical alloying and powder metallurgy(Ø60 × 3 mm). Magnetron sputtering (MSP-300B) was employed, with monocrystalline silicon wafer substrates used for the deposition of $FeCoNi(CuAl)_{0.2}$ films under an argon (Ar) atmosphere. Prior to deposition, the magnetron sputtering reaction vessel was evacuated to a residual cell pressure below 5 Pa and then filled with high-purity argon. The experimental parameters for the magnetron sputtering processes included a gas flow rate of 50 sccm, power input of 280 W, a substrate temperature of 500 °C and sputtering time 30 min.

The phase structures were investigated by using x-ray diffraction (XRD, Bruker D8 ADVANCE X-ray diffractometer with a Cu Kα radiation). Detailed microstructural characterization was performed using a scanning electron microscope (SEM) equipped with energy-dispersive spectroscopy (EDS) and an atomic force microscope (AFM). The magnetic behavior of both $FeCoNi(CuAl)_{0.2}$ target material and thin films were examined via a vibrating sample magnetometer (VSM, scanning the applied field between -15 kOe and +15 kOe) test at room temperature and under a magnetic field of 2.0 T.

* Corresponding author: S. Yang
E-mail: *yangshf@njit.edu.cn*

3. RESULTS AND DISCUSSION

The XRD pattern of the FeCoNi(CuAl)$_{0.2}$ HEA film is illustrated in Fig. 1. The result indicates that the FeCoNi(CuAl)$_{0.2}$ film is composed of a single solid solution phase (PDF#: 47-1405, FCC:Fe0.64Ni0.36).

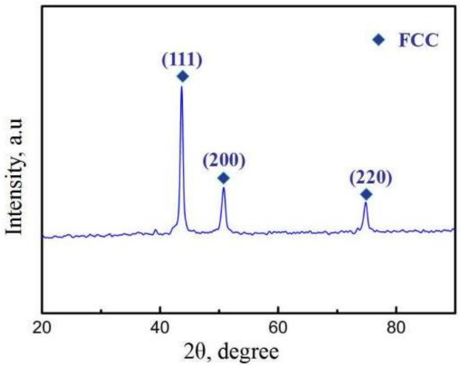

Fig. 1. XRD pattern of magnetron sputtering FeCoNi(CuAl)$_{0.2}$ HEA film

According to the formation theory of high entropy alloy, multi-principal component alloy has a high entropy effect and hysteresis diffusion effect, which are mainly based on mixing entropy (ΔS_{mix}), mixing enthalpy (ΔH_{mix}), and the valence electron concentration of the system. The relevant feature parameters of the FeCoNi(CuAl)$_{0.2}$ alloy system were calculated using the following equations [6–8]:

$$S_{mix} = -R \cdot \sum_{i=1}^{n} c_i \ln c_i; \quad (1)$$

$$\Delta H_{mix} = \sum_{i=1, i\neq j}^{n} \Omega_{ij} c_i c_j; \quad (2)$$

$$\Omega = \frac{T_m \Delta S_{mix}}{|\Delta H_{mix}|}; \quad (3)$$

$$VEC = \sum_{i=1}^{n} Ci(VEC)i\, \Omega_{ij} = 4\Delta H_{ij}^{mix}, \quad (4)$$

where ΔH_{mix} is the mixing enthalpy for the binary equiatomic ij alloys (Table 1); T_m (1324 °C) is the melting point of FeCoNi(CuAl)$_{0.2}$ alloy system, and $(VEC)_i$ is the VEC of valence electron component *i* of FeCoNi(CuAl)$_{0.2}$.

Table 1. The valence electron concentration and ΔHij_{mix} (kJ/mol) of FeCoNi(CuAl)$_{0.2}$ alloy [6]

Elements	Fe	Co	Ni	Al	Cu	$(VEC)_i$
Fe	-	-1	-2	-11	13	8
Co	-	-	0	-19	6	9
Ni	-	-	-	-22	4	10
Al	-	-	-	-	-1	3
Cu	-	-	-	-	-	11

The calculated results of ΔS_{mix}, ΔH_{ij}^{mix}, Ω, and VEC for FeCoNi(CuAl)$_{0.2}$ HEAs were shown as 11.71 J/mol, -3.31kJ/mol, 4.67, 8.87, respectively. These values align with available literature [6], indicating the formation of FeCoNi(CuAl)$_{0.2}$ film single FCC phase due to the BCC-structured solid solution, VEC < 6.8 and while for FCC, VEC > 8.

Fig. 2. shows SEM images of the magnetron-sputtered FeCoNi(CuAl)$_{0.2}$ HEA film. The results reveal that thin films obtained by sputtering exhibit the presence of columnar crystals with a thickness of approximately 0.72 µm after 30 min (Fig. 2 a). Energy-dispersive spectroscopy (EDS) analysis (Fig. 2 b) indicates that Fe, Co, Ni, Al, and Cu are uniformly distributed in the sputtered film. Fig. 3 a presents the surface of the magnetron-sputtered FeCoNi(CuAl)$_{0.2}$ HEA film and Fig. 3 b displaying AFM morphologies. The surface of the film exhibits a folded shape, and the film layer is relatively uniform. At the sputtering power of 280 W, FeCoNi(CuAl)$_{0.2}$ HEA film and Si substrate are closely bonded, and both show a dense columnar structure.

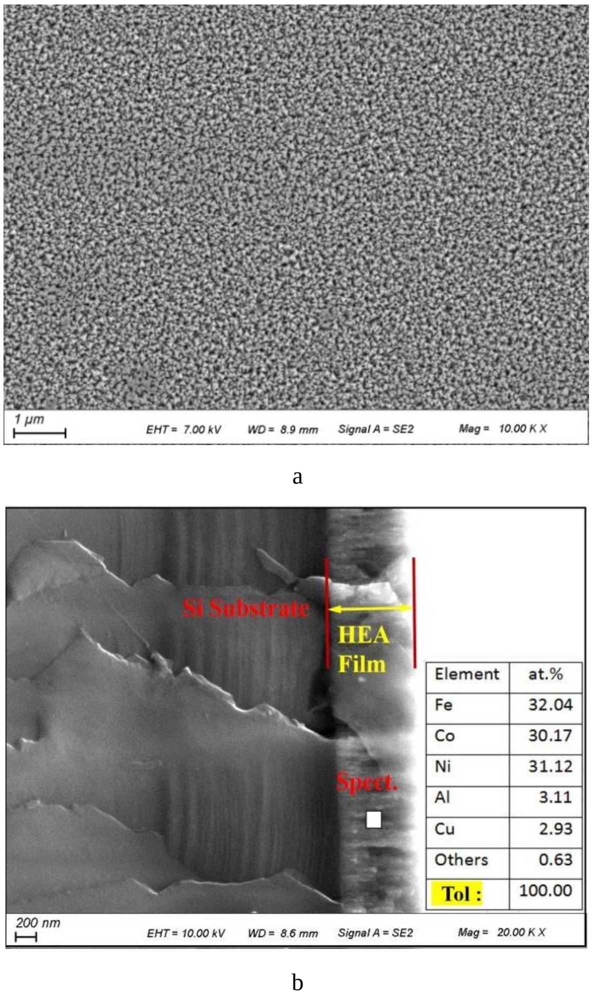

Fig. 2. a – SEM micrographs of FeCoNi(CuAl)$_{0.2}$ HEA film; b – EDS data for the cross-section

In the initial stage of film growth, the film crystals are fine and dense and grow in the direction close to the vertical base (Fig. 3 a inset). With the increase of film thickness, the film crystal particles become larger, and the columnar structure becomes wider. The average roughness (*R*a), root mean square roughness (*R*q), and maximum roughness (*R*max) are measured as 3.59 nm, 4.5 nm, and 37.5 nm, respectively (Fig. 3 b).

Fig. 4 presents the results of displacement-load, displacement-hardness curves and displacement-Young's modulus obtained by nanoindentation apparatus (NA). The hardness and Young's modulus are measured as 136.8 GPa and 7.33 GPa, respectively. These favorable mechanical stability properties are attributed to the atomic hysteresis diffusion effect in the high entropy alloy system, leading to a stable super solid solution formed by each element atom in the system. The element of Al with a large atomic radius in the alloy system increases the atomic radius difference ratio

$$(\delta= \sqrt{\sum_{i=1}^{n} c_i\left(1-{r_i}/{(\sum_{i=1}^{n} c_i r_i)}\right)^2}, \delta = 3.3\%)$$

of the system due to Aluminum has a large atomic radius (1.82 Å) relative to Fe, Co or Ni, causing a certain face-centered cubic solid solution lattice distortion [8]. This distortion enhances the film's deformation resistance and hardness.

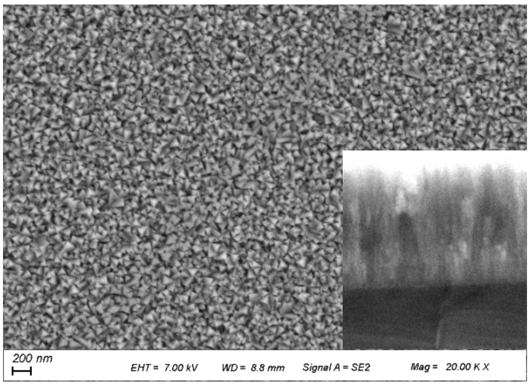

a

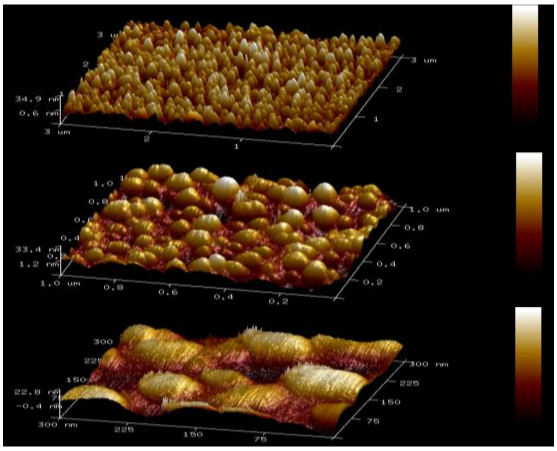

b

Fig. 3. a – SEM micrographs of $FeCoNi(CuAl)_{0.2}$ HEA film; b – upper surface with AFM three-dimensional diagram

Fig. 5 presents the magnetic properties of the $FeCoNi(CuAl)_{0.2}$ target material (blue line) and the thin films (red line). The thin $FeCoNi(CuAl)_{0.2}$ film displays excellent magnetic properties, which with a high MS of 139.67 emu/g and a low coercivity of 7.91 Oe. In contrast, the target material exhibits higher MS and lower MS values, measured at 104.7 Oe (Fig. 5 inset) and 125.4 emu/g, respectively. For the convenience of comparison, the magnetic properties of high-entropy alloys studied by others and this study are listed in Table 2. The magnetic properties of soft magnetic materials are influenced not only by the content of magnetic elements and crystal structure but also by grain size, crystal defects, and residual stress in the material [7, 8]. The content of ferromagnetic elements significantly impacts the average Bohr magneton ($\bar{\mu}_H$) of $FeCoNi(CuAl)_{0.2}$ HEA. The $\bar{\mu}_H$ can be counted by Eq. 5:

$$\bar{\mu}_H = \sum \mu_{H,i} \cdot x_i, \quad (5)$$

where $\mu_{H,i}$ is the Bohr magneton number of $FeCoNi(CuAl)_{0.2}$ HEA ($\mu_{H,Fe} = 2.2\mu_B$, $\mu_{H,Co} = 1.7\mu_B$, $\mu_{H,Ni} = 0.6\mu_B$ and $\mu_{H,Al} = 0\mu_B$); x_i is the atomic percentage of $FeCoNi(CuAl)_{0.2}$ HEA. The calculated values $\bar{\mu}_H$ is determined to be 1.4 μB per atom for the $FeCoNi(CuAl)_{0.2}$ alloy, which leads to a favourable MS for $FeCoNi(CuAl)_{0.2}$ HEA. In soft magnetic materials, when *D* (the grain size is larger) >Lex (the exchange length), the *Hc* is inversely proportional to grain size *D*, which can be calculated $FeCoNi(CuAl)_{0.2}$ HEA:

$$Hc = {p_c\sqrt{AK_1}}/{(\mu_0 M_s D)}. \quad (6)$$

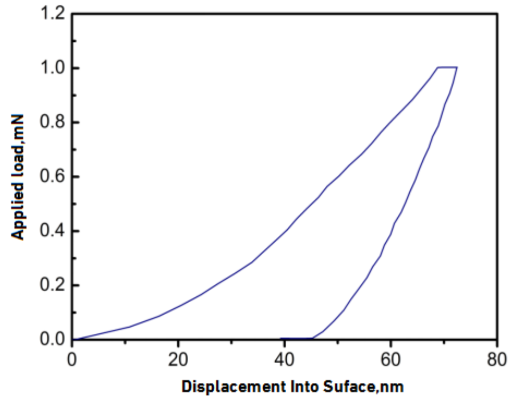

a

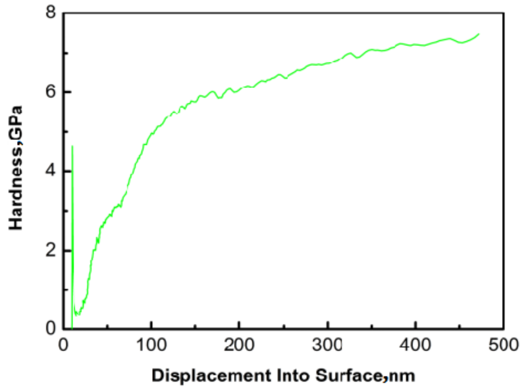

b

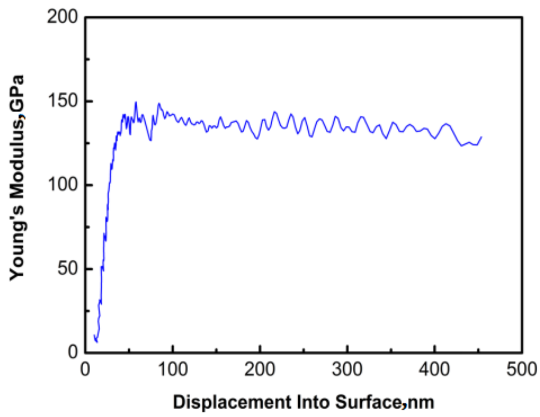

c

Fig. 4. The nano-indentation curves of $FeCoNi(CuAl)_{0.2}$ high entropy alloy films: a – displacement-load; b – displacement-hardness curves and c – displacement-Young's modulus

Table 2. Magnetic of $FeCoNi(CuAl)_{0.2}$ HEA film compared with the References

Composition, at.%	M_s, emu/g	H_c, Oe	Ref.
$(FeCoNi)_{70}Ti_{10}B_{20}$ powder 350 °C	119.2	13.4	[4]
CoNiMnGa arc melting	115.92	25	[14]
CuCrFeTiNi SPS-ed	64.38	4.63	[15]
CoCuFeMnNi powder	84	6	[16]
FeCoCuNiMn arc melting	40.64	346	[17]
CoCrFeCuNi HPS	53.41	166	[18]
$FeCoNi(CuAl)_{0.2}$ HEA film	139.67	7.96	This Study

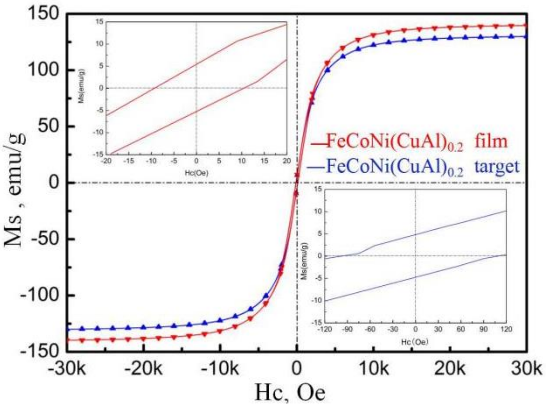

Fig. 5. Hysteresis loops of $FeCoNi(CuAl)_{0.2}$ HEA film and target.

As observed in Fig. 3 b., the magnetron sputtering film layer formed a columnar crystal structure growing perpendicular to the surface of the silicon substrate, with bigger grains having a average radial size at 72 nm under controlled formation parameters. Consider the larger Ms (139.67 emu/g) and the constants Pc(2.31), A(1.7 × 10-11 J/m), K1(1.5 × 104 J/m^3), μ0 (1.4). By substituting the above data into Eq. 6, the *Hc* can be calculated as *Hc* = 8.19, which is consistent with the measured experimental value (7.96 Oe). Additionally, due to the balanced growth of columnar crystal grains during the magnetron sputtering process, there is minimal internal stress and grain boundaries within each individual columnar crystal. These factors contribute to the excellent soft magnetic properties exhibited by the magnetron sputtering film. In contrast, the target sample consists of powder alloy obtained through high-temperature vacuum hot pressing, where the powder material undergoes non-equilibrium ball milling, resulting in significant internal stress [9 – 11]. Powder metallurgy solid forming leads to the formation of micron-sized grains with multiple grain boundaries in the target material. Coercive force in intrinsic magnetism of soft magnetic materials is closely related to the crystal structure and defects of the materials, and the coercive force will increase with large internal stress and multi-defect structural materials. Consequently, the coercivity of the target is higher, and the magnetic saturation (MS) is relatively lower compared to the magnetron sputtering film [12, 13].

4. CONCLUSIONS

$FeCoNi(CuAl)_{0.2}$ HEA films were fabricated using magnetron sputtering. The HEA film alloy exhibits a pure homogeneous face-centered cubic (FCC) structure, with a microstructure consisting of uniform 72 μm columnar crystals. The homogeneous solid solution phase and microstructure contribute to the alloy's high hardness, high modulus, and excellent soft magnetic properties. The measured values for hardness, Young's modulus, saturation magnetization, and coercivity are 136.8 GPa, 7.33 GPa, 139.67 emu/g, and 7.96 Oe, respectively, and which shows that the high entropy alloy films obtained by magnetron sputtering have superior magnetic properties and mechanical properties than $(FeCoNi)_{70}Ti_{10}B_{20}$, CoNiMnGa Arc melting, FeCoCuNiMn Arc melting and CoCrFeCuNi HPS (Table 2).

Acknowledgments

This study was supported by the Quzhou Science and Technology Research Competition Project(2024K193), the Fundamental Research Funds for Tianjin University of Technology and Education (KYQD202308) and the Opening Project of Guangdong Provincial Key Laboratory for Processing and Forming of Advanced Metallic Materials,South China University of Technology（GJ 202406).

REFERENCES

1. **Zeraati, M., Feizabad, M.H.K., Khayati ,G.R.** An Investigation of the Magnetic, Mechanical, and Kinetic Characteristics of CuCrFeTiNi High Entropy Alloy by Mechanical Alloying and Spark Plasma Sintering *Journal of Alloys Compounds* 958 2023: pp. 170347. https://doi.org/10.1016/j.jallcom.2023.170347
2. **Kumari, P., Gupta, A.K., Mishra, R.K., Ahmad, M.S.** A Comprehensive Review: Recent Progress on Magnetic High Entropy Alloys and Oxides *Journal of Magnetism and Magnetic Materials* 554 2022: pp. 169142. https://doi.org/10.1016/j.jmmm.2022.169142
3. **Kang, T.X., Wu, S.Y., Wang, M.L., Lu, Y.P.** Novel $Fe_2CoNi(AlSi)x$ High-entropy Alloys with Attractive Soft Magnetic and Mechanical Properties *Applied Physics A* 127 2021: pp. 829. https://doi.org/10.1007/s00339-021-04988-7
4. **Bora, K., Tuncay, S., Baris, A.** Atomic Configurations in Mechanically Alloyed Amorphous $(FeCoNi)_{70}Ti_{10}B_{20}$ Powders *Journal of Alloys and Compounds* 960 2023: pp. 170667. https://doi.org/10.1016/j.jallcom.2023.170667
5. **Chaudhary, V., Chaudhary, R., Banerjee, R.** Accelerated and Conventional Development of Magnetic High Entropy Alloys *Materials Today* 49 2021: pp. 231 – 252. https://doi.org/10.1016/j.mattod.2021.03.018
6. **Zhang, Y., Zuo, T.T., Tang, Z., Gao, M.C., Dahmen, K.A., Liaw, P.K., Lu, Z.P.** Microstructures and Properties of High-entropy Alloys *Progress in Materials Science* 61 2014: pp. 1 – 93.

http://dx.doi.org/10.1016/j.pmatsci.2013.10.001

7. **Chen, H.Y., Gou, J.M., Jia, W.T., Song, X., Ma, T.Y.** Origin of Hard Magnetism in Fe-Co-Ni-Al-Ti-Cu High-entropy Alloy: Chemical Shape Anisotropy *Acta Materiala* 246 2023: pp. 118702. https://doi.org/10.1016/j.actamat.2023.118702
8. **Sahu, P., Samal, S., Kumar, V.** Microstructural, Magnetic, and Geometrical Thermodynamic Investigation of FeCoNi(MnSi)x (0.0, 0.1, 0.25, 0.5, 0.75, 1.0) High Entropy Alloys *Materialia* 18 2021: pp. 101133. https://doi.org/10.1016/j.mtla.2021.101133
9. **Zhou, K.X., Sun, B.R., Liu, G.Y., Li, X.W., Xin, S.W., Liaw, P.K., Shen, T.D.** FeCoNiAlSi High Entropy Alloys with Exceptional Fundamental and Application-oriented Magnetism *Intermetallics* 122 2020: pp. 106801. https://doi.org/10.1016/j.intermet.2020.106801
10. **Javdan, M., Gheisari, K., Reihanian, M.** Mechanically Alloyed $(FeCoNi)_{75}Cu_{25-x}Si_x$ hHigh Entropy Alloys: Phase Evaluation and Magnetic Properties *Journal of Alloys Compounds* 952 2023: pp. 170030. https://doi.org/10.1016/j.jallcom.2023.170030
11. **Gao, W., Dong, Y.Q., Jia, X.J., Yang, L.P., lI, X.B., Wu, S.D., Zhao, R.L., Wu, H., Li, Q., He, A.N., Li, J.W.** Novel CoFeAlMn High-entropy Alloys with Excellent Soft Magnetic Properties and High Thermal Stability *Journal of Materials Science & Technology* 153 2023: pp. 22 – 31. https://doi.org/10.1016/j.jmst.2023.01.010
12. **Jahani, N., Reihanian, M., Gheisar, K.** Alloying, Phases and Magnetic Behaviour of Mechanically Alloyed FeNiMnCu-based High Entropy Alloys *Materials Science and Technology* 39 2023: pp. 1745 – 1759. https://doi.org/10.1080/02670836.2023.2180902
13. **Han, L., Maccari, F., Filho, I.R.S., Peter, N.J., Wei, Y., Gault, B., Gutfleisch, O., Li, Z., Rabbe, D.** A Mechanically Strong and Ductile Soft Magnet with Extremely Low Coercivity *Nature* 608 2022: pp. 310 – 316. https://doi.org/10.1038/s41586-022-04935-3
14. **Zuo, T.T., Zhang, M., Liaw, P.K., Zhang, Y.** Processing Effects on the Magnetic and Mechanical Properties of $FeCoNiAl_{0.2}Si_{0.2}$ High Entropy Alloys *International Journal of Minerals Metallurgy and Materials* 20 2013: pp. 549 – 551. https://doi.org/10.1007/s12613-013-0764-x
15. **Talaat, A., Suraj, M.V., Byerly, K., Wang, A.Y., Wang, A., Lee, J.K., Ohodnicki, P.R.** Review on Soft Magnetic Metal and Inorganic Oxide Nanocomposites for Power Applications *Journal of Alloys and Compounds* 870 2021: pp. 159500. https://doi.org/10.1016/j.jallcom.2021.159500
16. **Zhao, R.F., Ren, B., Zhang, G.P., Liu, Z.X., Zhang, J.J.** Effect of Co Ccontent on the Phase Transition and Magnetic Properties of CoxCrCuFeMnNi High-entropy Alloy Powders *Journal of Magnetism and Magnetic Materials* 468 2018: pp. 14 – 24. https://doi.org/10 .1016/j.jmmm.2018.07.072
17. **Kürşat, I.** Investigation of Phase Transformation Related Magnetic Properties of Ti Addition to FeCoCuNiMn and FeCoCuNiAl High Entropy Alloys by Vacuum Arc Melting *Materials Today Communication* 39 2024: pp. 108821. https://doi.org/10.1016/j.mtcomm.2024.108821
18. **Mishra, R.K., Shahi, R.** A Systematic Approach for Enhancing Magnetic Properties of CoCrFeNiTi-based High Entropy Alloys Via Stoichiometric Variation and Annealing *Journal of Alloys and Compounds* 821 2020: pp. 153534. https://doi.org/10.1016/j.jallcom.2019.153534